Land Cover Change Detection and Analysis of Mts. Palay-Palay Mataas-Na-Gulod Protected Landscape, Philippines using Satellite Imagery

Mitsui Chin Sen A. Yu* and Jan Joseph V. Dida
Institute of Renewable Natural Resources
University of the Philippines Los Baños
College, Laguna 4031 Philippines
*mayu4@up.edu.ph

Date received: July 14, 2022
Revision accepted: January 5, 2023

Abstract

Several studies have already proven the existence of unsustainable human activities or disturbances assumed to cause land cover change on the Mts. Palay-Palay Mataas-Na-Gulod Protected Landscape (MPPMNGPL)in the Philippines. However, there is a dearth of published works on how these disturbances affect the different land cover classes in this protected landscape. This study aimed to help fill such information gap by investigating the extent of land cover changes and potentially disturbed forest areas inside the MPPMNGPL. Using geographic information system and remote sensing, classified maps were produced from Sentinel-2 and Landsat-8 images through supervised classification. The study described the land cover types and land cover changes in the area from 2015 to 2021 and identified potentially disturbed forest areas using the normalized difference moisture index (NDMI). The land cover classes identified in the area included forest, grassland, built-up, barren land and water. From 2015 to 2021, the largest land cover change came from the 510.92 ha of forest area in Ternate that turned into a grassland area as reflected in the NDMI result – an indicator of potential forest disturbance. Change detection showed that from 2015 to 2021, the grassland area had an increase of +14.05%, while the forest area had a decrease of -13.8%. Results showed that forest is still the most dominant land cover class in the protected landscape. Further studies and ground validation must be conducted to determine the specific causes of the land cover changes.

***Keywords**:* image classification, normalized difference moisture index, protected area, remote sensing, Sentinel-2

1. Introduction

In the Philippines, land cover changes are inevitable in urbanizing areas and even within protected areas. A nationwide forest cover assessment from 2000 to 2012 showed that many terrestrial protected areas in the Philippines had

encountered drastic forest cover loss (Apan *et al*., 2017). The same study revealed that some of the protected areas with the largest forest loss area have high rates of forest loss within their buffer zones. Soriano *et al*. (2019) assessed the land use/land cover (LULC) and urban sprawl in the Mount Makiling Forest Reserve Watersheds and buffer zone from 1992 to 2015. Results showed that LULC change happened when built-up areas increased by 117% despite the regulations implemented. In addition, LULC monitoring at the Mt. Pulag National Park from 1990 to 2020 disclosed an increase in agricultural and built-up areas and a decrease in forest areas indicating that human-induced land cover changes were causes of forest loss (Doyog *et al*., 2021). Lastly, at the Allah Valley Protected Landscape in South Cotabato, trends in land cover change detected from 1989 to 2015 showed a decreasing forest area and increasing agricultural, grassland and built-up areas (Janiola and Puno, 2018). Changes in the physical characteristics of the land cover, including the distribution of vegetation, water, soil and other physical features catalyzed by natural or anthropogenic factors, result in land cover changes (Yadav *et al*., 2019). The impetus for land cover changes has been attributed to the direct drivers of deforestation including unsustainable forest product extraction, agricultural expansion and infrastructure construction (Carandang *et al*., 2013).

The Mts. Palay-Palay Mataas-Na-Gulod Protected Landscape (MPPMNGPL) was declared a protected area in 2007 through Proclamation No. 1315, s. 2007, under the National Integrated Protected Areas System (NIPAS) Act of 1992 and one of the key conservation sites in the Philippines (Mallari and Tabaranza, 2001). Like other protected areas, it has experienced forest disturbance due to land cover changes. Studies have recorded anthropogenic activities in the area including harvesting non-timber forest products, charcoal manufacturing, quarrying, cow grazing and logging within the strict protection zone (SPZ). Human encroachment, which can contribute to the manifestation of land cover changes, has also been documented in the MPPMNGPL (Angeles *et al*., 2016; Causaren *et al*., 2016).

However, the extent of land cover change in MPPMNGPL has not been examined. Hence, there is a need to describe the extent of land cover changes. Moreover, potentially disturbed areas in the protected landscape must be determined using geographic information system (GIS) and remote sensing (RS) since traditional mapping techniques such as manual cartography, sketch mapping, or pen-and-paper sketching are time-consuming, costly and cannot possibly illustrate and quantify spatial and temporal changes (Baamonde *et*

al., 2019; Verma and Garg, 2019). These technologies have become the common approach in land cover change analysis and detection (Abino *et al*., 2015; Apan *et al*., 2017; Haque and Basak, 2017; Yadav *et al*., 2019). Remote sensing, combined with GIS, can facilitate digital change detection by capturing a larger view of the area of interest without physical contact using remotely sensed data observing the earth's surface features and detecting spatial changes from multi-temporal satellite images more clearly in other applications (Alqurashi and Kumar, 2013; Halefom *et al*., 2018; Asokan and Anitha, 2019). Recent studies have proven the effectiveness of GIS and the use of remotely sensed images in facilitating the detection, analysis and prediction of land cover changes in different areas around the world (Barakat *et al*., 2018; Eskandari *et al*., 2020; Sánchez-Espinosa and Schröder, 2019; Thanh *et al*., 2020). Essentially, they allow for time-saving and less expensive methods pertinent to the study including the acquisition of satellite images with different temporal, spatial and spectral resolutions; image classification to produce reliable maps presenting the different land cover classes; and use of vegetation index to identify potentially disturbed areas. Moreover, it has become more important to utilize these technologies as it was difficult to reach and access the protected landscape due to the restrictions caused by the COVID-19 pandemic.

The semi-automatic classification plugin (SCP) offers tools that can facilitate the different phases from acquisition to post-processing of remotely sensed data and specifically ease the image classification processes (Congedo, 2021). Image classification can be done through supervised or unsupervised classification. In supervised classification, training sets or identical pixels within the image are visually selected and assigned to pre-determined classes (e.g., forest, built-up and water) representing the pixels (Perumal and Bhaskaran, 2010). Moreover, this can be done following a series of processes, namely defining the training sets, extractions of signatures and classification of the image. Prior knowledge about the site increases the accuracy of this method (Yiqiang *et al*., 2010). Shah and Kiran (2021) claimed that supervised classification was a versatile, useful and easy-to-use method for land cover change detection.

It is also a common approach in several studies related to land cover change detection conducted in the Philippines (Dumago *et al*., 2018; Soriano *et al*., 2019; Almadrones-Reyes and Damagac, 2022). Spectral angle mapper (SAM) is one of the available classification algorithms from the SCP. Kruse (1994) stated that the SAM algorithm is the most basic approach to producing a map

demonstrating the spatial distribution of its materials by empirically matching the two spectra considering the determined spectral similarity. Anggraeni and Lin (2011) employed the SAM algorithm as one of the techniques to measure fire-induced deforestation in South Sumatra, Indonesia. Brebante (2017) has also used this in LULC change detection in Marikina River Basin, Philippines. The normalized difference moisture index (NDMI) measures the vegetation water content and is known for its high correlation with the canopy water content (United States Geological Survey, 2021; Klemas and Smart, 1983). Studies have found that NDMI as a vegetation index is suitable for detecting vegetation disturbances. In Wilson and Sader (2002), it was found through classification trials that NDMI is more accurate than the normalized difference vegetation index (NDVI), which is a more commonly used method. Its accuracy is due to its greater sensitivity to vegetation disturbances and resistance to data noise than the other vegetation indices (Ochtyra *et al*., 2020). These technologies provide detailed information that helps researchers understand the condition of protected areas, which can then serve as a basis for making recommendations regarding their management.

The general objective of this study was to assess the extent of land cover changes and identify potentially disturbed areas in MPPMNGPL from 2015 to 2021 using satellite imagery. The study specifically aimed to determine various land cover classes, describe the land cover changes and identify forest areas within the protected landscape that are potentially disturbed.

2. Methodology

2.1 Description of the Study Site

MPPMNGPL spans 3,973.13 ha or approximately 4,000 ha within the municipalities of Maragondon and Ternate in Cavite and Nasugbu in Batangas, Philippines (Figure 1) with geographic coordinates of 14° 16’ 58.432” N latitude and 120° 51’ 49.227” E longitude. It is the only protected area in the province of Cavite. The area has become popular among many hikers and mountain climbers (Municipality of Maragondon, 2013). Based on rainfall distribution, MPPMNGPL is under the Type 1 climate. Under this type, there are two well-defined seasons based on rainfall and temperature: dry from November to April and wet from May to October wherein the maximum rain period can be experienced from June to September (Philippine Atmospheric, Geophysical and Astronomical Services Administration, n.d.).

It has three peaks located on Pico de Loro (595 masl), Mataas Na Gulod (622 masl), and Palay-Palay (647 masl) (Causaren, 2016). In 1975, by Proclamation No. 1520, the Municipalities of Maragondon and Ternate in Cavite and the Municipality of Nasugbu in Batangas were declared tourist zones. The proclamation allowed the Philippine Tourism Authority to identify areas with high tourism values where development efforts from both the government and private sectors can be implemented to generate tourist receipts and foreign exchange. According to the Cavite Ecological Profile (2020), the MPPMNG was developed into an eco-tourism spot because of its vast floral and faunal assemblage despite the unresolved issues regarding the imbalances in its exploration and conservation. As indicated in the 2010-2020 Comprehensive Land Use Plan (CLUP) of Ternate (Municipality of Ternate, n.d.), big tourism resorts such as the Puerto Azul Beach Resort and Hotel and Caylabne Bay Resort were developed inside the protected landscape resulting in some boundary conflicts. With that, it has become a region of interest because despite being proclaimed a key biodiversity hotspot and protected area in 2007, most recent studies confirmed that anthropogenic activities and disturbances still exist within its boundaries (Angeles *et al*., 2016; Causaren *et al*., 2016; Cavite Ecological Profile, 2020).

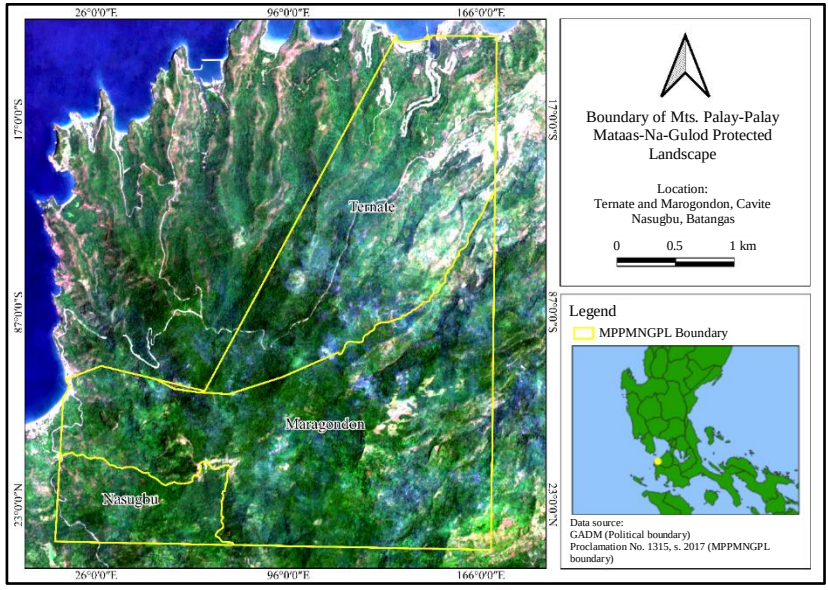

Figure 1. Location map of the study area; true-color Sentinel-2 image of MPPMNGPL using bands 4, 3 and 2

According to the Esri 2020 land cover classification (Table 1) (Esri, 2022), the land cover types in the area include forest land, grassland, built-up area, barren land and water. The estimated forested area is 62.5%, and the non-forested is 37.5% (Causaren, 2016). This forest was classified as a secondary growth forest of molave-dipterocarp type where premium tree species such as *Albizia acle*, *Vitex parviflora*, *Diospyros blancoi*, *Shorea negrosensis*, *Shorea contorta*, *Shorea guiso*, *Canarium ovatum* and *Cinnamomum mercadoi* can be found. A faunal diversity assessment conducted in 1995 by the Professional Environmental Management Company showed that 124 wildlife species were identified in the area (National Economic and Development Authority, 2008). Based on a floral assessment conducted by Medecilo and Lagat (2017), the most dominant species with the highest importance value index in the protected landscape are *S. guiso*, *Ficus chrysolepis* and *Diospyros pyrrhocarpa*. The reported remaining lowland evergreen rainforest of Cavite is located in the northern portion of the protected landscape on Mt. Palay-Palay (Municipality of Maragondon, 2013). There were virtually no land cover change analysis and detection studies previously done in the protected landscape.

Table 1. Definition of land cover classes based on ESRI 2020 land cover

Land cover class	Definition
Forest land	Area with significant clustering of tall (approximately 15 m or higher) and dense vegetation in a closed or open canopy; this includes closed and open canopy forests.
Grassland	Open areas covered with homogeneous grasses mixed with sporadic and small clusters of shrubs and tree growths; and shrub-filled clearings within forests that are not taller than trees
Built-up area	Area either rural or urban with man-made structures such as residential housings, buildings, parking structures, major roads, rail networks and other infrastructures
Barren land	Area that shows exposed rock or soil with very little to no vegetation for the entire year
Water	Area where water is predominantly present for the entire year; it contains little to no sporadic and small clusters of vegetation. It does not include areas with sporadic or ephemeral water and built-up structures like docks.

2.2 Data Collection and Pre-Processing

In this study, Sentinel-2 MSI: Level-1C satellite imagery was obtained from the Earth Engine Data Catalog of Google Earth Engine (GEE). GEE is a free cloud-based computational platform using Google Cloud and JavaScript

language to access and process petabyte scales of satellite data (Praticò *et al*., 2021). Sentinel-2 imagery performs better than Landsat-8 imagery in vegetation analysis due to its finer spatial resolution (Chaves *et al*., 2020) and improved spectral and temporal resolutions (Sánchez-Espinosa and Schröder, 2019). Due to its higher spatial resolution than Landsat-8, mapping small disturbances became possible making it more effective in delineating log landings and filling gaps than Landsat-8 data (Lima *et al*., 2019).

The selection and use of 2015 Landsat-8 C1 T1 satellite imagery from the same platform was necessary because the Sentinel-2 imagery covering the study site for 2015 was very cloudy causing an error in the processing. Even though Landsat-8 imagery has a lower resolution than Sentinel-2, it has been used in many published studies related to land cover change analysis in protected areas such as by Soriano *et al*. (2019) and Janiola and Puno (2018). The details of the satellite data sources of 2015, 2018 and 2021 images were provided (Korhonen *et al*., 2017; Li and Roy, 2017; Wang *et al*., 2018) (Table 2).

Table 2. Details of the satellite data sources of the acquired satellite images

Parameters	Acquired satellite images	
	2015	2018 and 2021
Platform	Landsat-8	Sentinel-2
Satellite sensor	Operational land imager (OLI)/ Thermal infrared sensor (TIRS)	Multi-spectral instrument (MSI)
Spectral bands	7	13
Spatial resolution	30 m	10/20/60 m
Radiometric resolution	16 bits	12 bits
Temporal resolution	16 days	10 days
Availability	Open source 2013-03-18 to present	Open source 2015-06-23 to present

Several variables were specified to filter the image collection such as the area of interest (AOI), time interval and cloud percentage. A polygon was created in the GEE code editor to set the AOI boundary while ensuring that MPPMNGPL was entirely covered. Three different time periods with the following temporal filters were used: 2015 (2015-01-01, 2016-12-31), 2018 (2018-01-01, 2018-12-31) and 2021 (2020-01-01, 2021-12-31). Images with less than 10 and 5% cloud pixel percentages for Sentinel-2 and Landsat-8, respectively, were extracted.

The GEE code editor performed atmospheric correction for the acquired images except for the Landsat-8 image as it was imported from a dataset that was already atmospherically corrected. Cloud masking within the temporal filters was also done in the code editor. The extent of the GEE processing was confined to the AOI boundary. Finally, the spatial resolution was set to 10 m for Sentinel-2 images and 30 m for Landsat-8 images. The three images from 2015 (Landsat-8), 2018 (Sentinel-2) and 2021 (Sentinel-2) were exported to Google Drive. A naming convention for the acquired images was created conveying the satellite data source, date of acquisition (YYYY/MM/DD), cloud pixel percentage, location and temporal filter used (Table 3).

Table 3. File names of the satellite images following a specified file naming convention

Satellite image	File name
2015 Landsat-8 image	L8_2022/03/04_5_MPPMNGPL_2015/01/01-2016/12/31
2018 Sentinel-2 image	S2_2022/03/08_10_ MPPMNGPL_2018/01/01-2018/12/31
2021 Sentinel-2 image	S2_2022/03/08_10_ MPPMNGPL_2020/01/01-2021/12/31

2.3 Image Classification and Accuracy Assessment

Using the 2015 (Landsat-8), 2018 (Sentinel-2) and 2021(Sentinel-2) images, three classified maps were generated through supervised classification using the SCP in QGIS v.3.16 (QGIS Development Team, 2020). As required by the SCP, bands 1, 2, 3, 4, 5, 6 and 7 of Landsat-8 image, and bands 1, 2, 3, 4, 5, 6, 7, 8, 8A, 9, 10, 11 and 12 of Sentinel-2 images were used in the image classification. Although other classification algorithms can be used, the SAM algorithm was employed to classify land cover classes as it is the most basic and available in the SCP. This algorithm assigns a particular pixel to represent a specific class depending on the determined spectral similarity between two pixels. This similarity is obtained by measuring the cosine of the angle between the two-pixel vectors (Tu *et al*., 2018; Yan and Roy, 2018). Verma *et al*. (2020) determined the best algorithm for LULC analysis among five parametric and nonparametric algorithms. The performance of SAM recorded the highest overall agreement and the most minor quantitative errors proving that it is the most accurate among the algorithms for LULC analysis.

At least 30 regions of interest (ROIs) were created for each land cover type. It should be noted that each ROI contains a different number of pixels as the

land cover types greatly differ in size (Figure 2). The classification report in the SCP determined the total areas and percentages of each land cover type. An accuracy assessment was performed on each classified map using at least 150 reference points from Google Earth Pro v. 7.3.2 (Google, 2022).

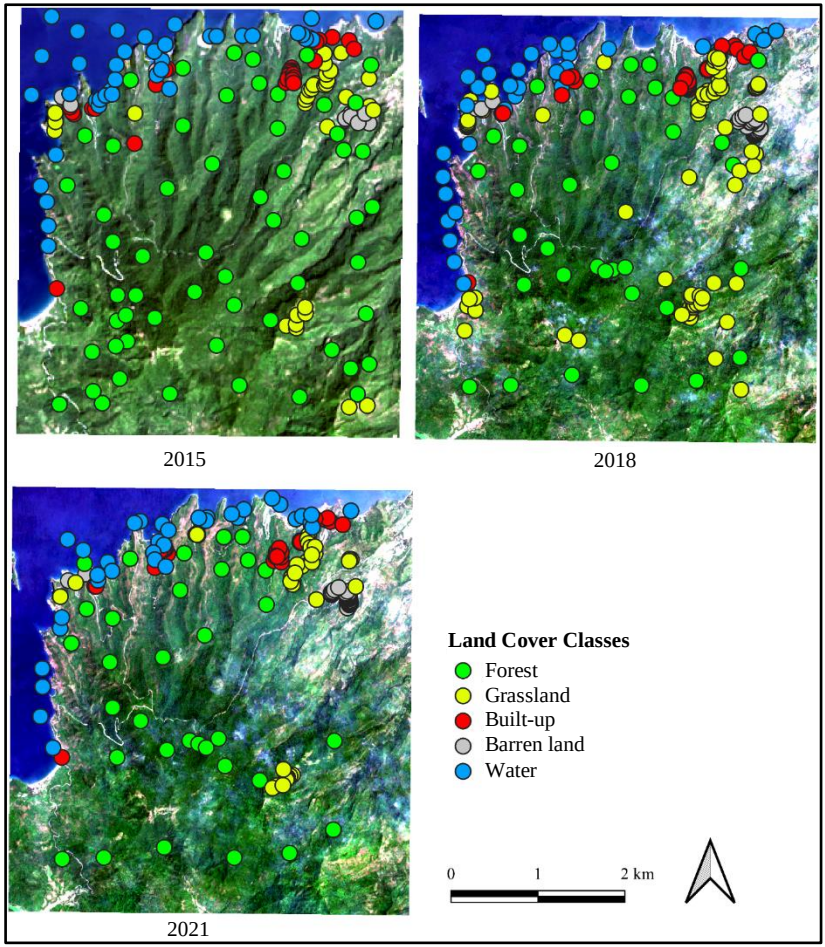

Figure 2. Vector layer displaying the generated ROIs for years 2015, 2018 and 2021

The accuracy assessment was based on the calculation of a confusion matrix presenting the comparison of mapped information with reference data for the identified ROIs to determine the accuracy of the classification (Congalton and Green, 2019). Accuracy parameters from the confusion matrix were the producer's accuracy, the user's accuracy, the overall accuracy and the kappa coefficient. The producer's accuracy was calculated for each land cover class

by dividing the number of correctly classified sites that matched the reference sites by the total number of reference sites for that class (Equation 1) (Liu *et al*., 2007). The user's accuracy was computed by dividing the number of correctly classified sites in a class by the total number of sites classified in the same class (Equation 2) (Grigoraș and Uriţescu, 2019). The overall accuracy was calculated by dividing the total number of correctly classified sites by the total number of reference sites (Equation 3). The kappa coefficient indicates the agreement between the classified image and the reality (Equation 4).

$$P_i = \frac{a_i}{x_i} \tag{1}$$

$$U_i = \frac{a_i}{y_i} \tag{2}$$

$$O = \frac{\sum_{i=1}^{8} a_i}{N} \tag{3}$$

$$Kappa = \frac{N\sum_{i=1}^{C} a_i - \sum(x_i y_i)}{N^2 - \sum(x_i y_i)} \tag{4}$$

Here, i represents the class of reference sites; a_i is the number of correctly classified sites; x_i indicates the total number of reference sites of a class; y_i corresponds to the total number of sites classified in the same class; N represents the total number of reference sites; and C is the number of classes. After ensuring that the classified maps were valid and accurate, the land cover change analysis was carried out through the SCP.

2.4 Identification of Potentially Disturbed Areas

The selection of an appropriate vegetation index is essential in identifying potentially disturbed areas. The NDMI was used to determine the forest areas within the study site that were potentially disturbed. The NDMI formulas for Sentinel-2 and Landsat-8 data are represented in Equations 5 and 6, respectively.

$$NDMI = \frac{B_8 - B_{11}}{B_8 + B_{11}} \tag{5}$$

$$NDMI = \frac{B_5 - B_6}{B_5 + B_6} \tag{6}$$

where B_8 (Sentinel 2) and B_5 (Landsat-8) are the near-infrared (NIR) band, and B_{11} (Sentinel 2) and B_6 (Landsat-8) are the shortwave infrared (SWIR) band. The index has the ability to determine vegetation water content by the combination of NIR and SWIR bands which can remove variations from the leaf's internal structure and leaf's dry matter content (Ceccato *et al*., 2001). This index has been used in the monitoring of forest disturbances in Afromontane Forest in Kenya (Brandt *et al*., 2018), forest degradation, deforestation and regeneration detection in montane forests of Eastern Tanzania (Hamunyela *et al*., 2020) and tropical forest disturbance monitoring in Tanzania and Brazil (Chen *et al*., 2021).

3. Results and Discussion

3.1 Land Cover Classification and Accuracy

Based on the image classification, MPPMNGPL was predominantly covered by forest followed by grassland (Figure 3). From 2015 to 2021, the land cover classes found in Maragondon were forest, grassland and built-up area, with forest dominating the protected landscape. In Ternate, the land cover classes identified were forest, grassland, built-up area, barren land and water. On the other hand, in Nasugbu, only forest and grassland were the classes identified.

Forest cover (80.97%) was present in all three municipalities, wherein Ternate and Maragondon had the largest forest areas. Grassland (18.08%) was also found in the three municipalities and was most abundant in Ternate. Built-up areas (0.56%) were found mainly in Ternate, smaller patches in Maragondon, and none in Nasugbu. Barren lands (0.20%) were present only in Ternate mainly concentrated in a previous and inoperative mining/quarry site and its peripheral area. Water bodies (0.23%) were found in Ternate and Maragondon. These were situated along the edge and boundary of the protected area and were very minimal in size. As shown in the classified maps, MPPMNGPL was generally covered by forest from 2015 to 2021 followed by grassland as the second largest class. The built-up area, barren land, and water were significantly smaller as they only covered less than 1% of the protected landscape.

The change detection showed that the forest and barren land decreased over time, with the forest having the largest decrease, from 94.77 in 2015 to 80.97%

in 2021 (Figure 4). On the other hand, grassland, built-up area and water increased over time. From 4.03 to 18.08%, grassland had the largest increase in area. Across the years, forest and barren land had a decrease of -13.8 and -0.46%, respectively. In contrast, grassland, built-up area and water had incurred a +14.05, +0.11 and +0.14% increase, respectively. No studies were found that can explain why the water has been increasing in the protected landscape. The use of images from different satellite data sources can be a probable reason; nevertheless, the percentage of change in the water was very minimal.

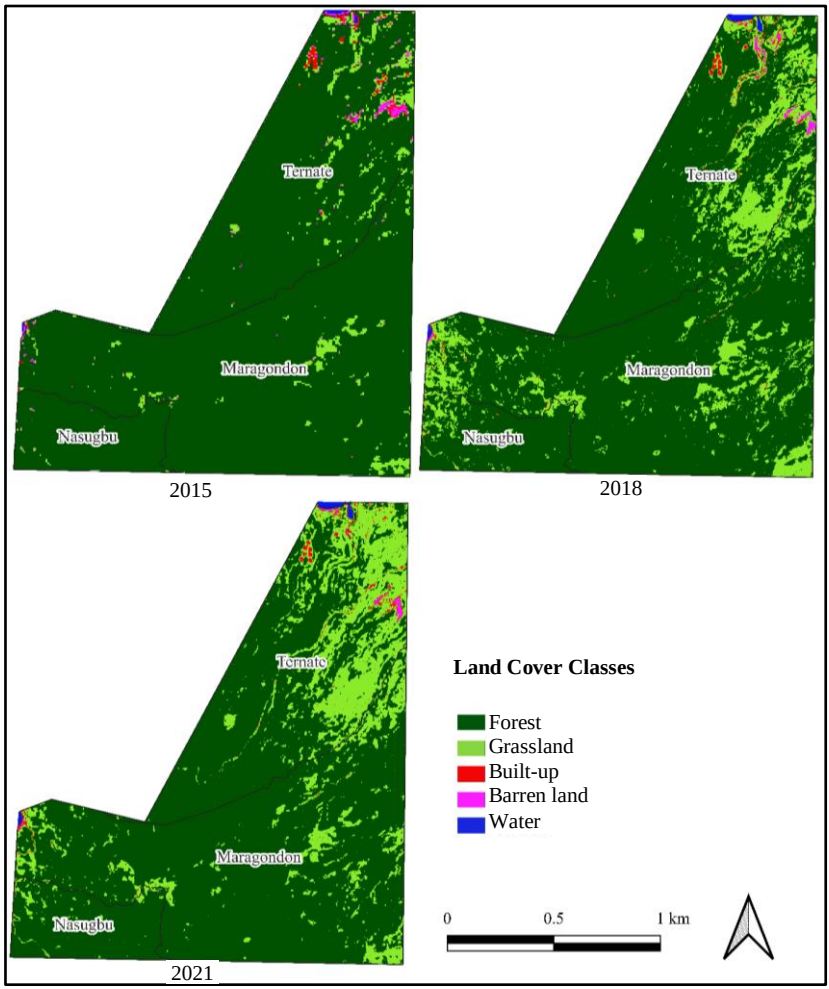

Figure 3. Classified Land Cover of MPPMNGPL in 2015, 2018 and 2021

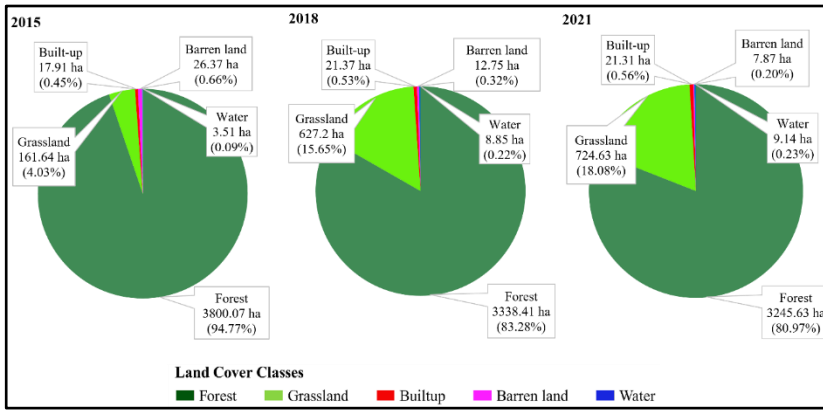

Figure 4. Areas in percentages of each land cover class from 2015, 2018 and 2021

Table 4 presents the summary of the producer and user's accuracies, kappa coefficient and overall accuracy of each classified image. According to Thomlinson *et al*. (1999), the acceptable minimum overall accuracy for land classification is 85%, while for Congalton (1991), it should not be less than 70%. In this regard, the accuracy assessment for all the classified images was acceptable.

Table 4. Summary of the confusion matrix of the 2015, 2018 and 2021 classified images

Classified image	Producer's accuracy (%)	User's accuracy (%)	Kappa coefficient	Overall accuracy (%)
2015	100	88.24	0.74	89.61
2018	99.34	96.74	0.93	96.51
2021	100	96.77	0.94	96.78

3.2 Land Cover Changes

Generally, the 2015-2018 and 2018-2021 land cover change maps have shown almost the same results because most changes have occurred in the same areas (Figure 5). Specifically, most of the land cover changes happened in Ternate followed by Maragondon and the least in Nasugbu. The largest land cover change happened to some 510.92 ha (2015-2018) and 410.22 ha (2018-2021) of forest area in Ternate that turned into a grassland (Figure 6). A total of 58.54 ha of grassland became forest from 2015-2018. Some built-up areas and

barren lands likewise turned into grassland areas. It was also seen that 13 ha of forests in 2015-2018 and 9.55 ha of grassland in 2018-2021 had been turned into built-up areas. Other land cover changes had occurred; however, they were very minimal compared to the changes in the grassland area.

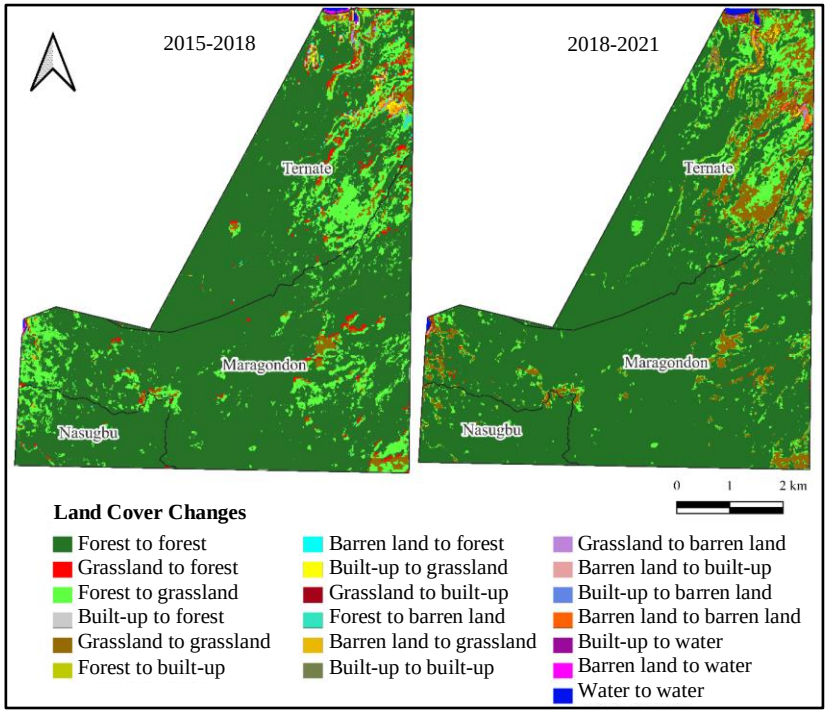

Figure 5. 2015-2018 and 2018-2021 land cover changes maps of MPPMNGPL

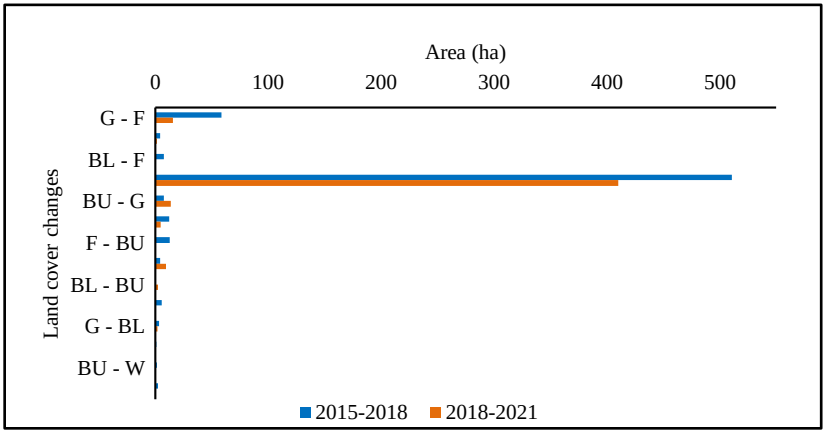

Figure 6. 2015-2018 and 2018-2021 land cover changes

According to the 2010-2020 CLUP of Ternate (Municipality of Tarnate, n.d.), some open grassland spread even within the forest and to areas with more than 18% slope. Moreover, the CLUP documented occasional exploitation through *kaingin* and logging activities leading to the denudation of some portions of the forest. Causaren *et al*. (2016) stated that in Cavite, grasslands can usually be found on the edges of its remaining forest fragments. Several anthropogenic threats were observed in the forest fragments in Mt. Palay-Palay. The most common threat was the conversion of forests to agricultural and residential lands (Lagat and Causaren, 2019). It can be a significant cause for the spread of the grassland area into the forest; hence, the increasing grassland area over time.

Some areas inside MPPMNGPL have been designated for small settlements, rural gardens and *kaingin* (Municipality of Maragondon, 2013). Due to tourism and other activities, threats were observed from the construction of resorts and highways and the settlers' encroachment (Medecilo and Lagat, 2017). In addition, it was stated in the Cavite Ecological Profile 2020 that illegal cutting of trees, encroachment of informal settlers and unsustainable activities caused deforestation even within the protected landscape (Province of Cavite, 2020).

The 2010-2020 CLUP of Ternate also documented a report by the Department of Environment and Natural Resources (DENR) of a quarry site inside the protected landscape shown in the classification as a contiguous barren land. The change detection showed that this area transitioned into grassland. As per the DENR Mines and Geosciences Bureau (DENR-MGB) Region 4-A (2021), mining companies have planted 52,265 seedlings as of 2015 in more than 7.85 ha of mined-out areas in Cavite. This activity needs to be verified on the ground, however. It is important to confirm whether the reforestation activity contributed to the conversion of the contiguous barren land caused by previous mining/quarrying activities into grassland and forest areas over time.

Changes in forest and barren land have caused an increase in grassland areas. In particular, the forest has recorded the largest land cover change in both periods contributing to the creation of new grasslands.

3.3 Potentially Disturbed Areas

The results of the NDMI from the three different years are presented in Figure 7. NDMI can only have values between negative 1 and positive 1 wherein the

negative values indicate that the area is disturbed. In contrast, the positive values indicate no water stress or undisturbed area. Here, the red pixels represent a relatively low vegetation water content, while the blue pixels represent high vegetation water content. The intervals and interpretations of values were defined following the study of Berca and Horoiaș (2022) and the index provided by Agricolus (Antognelli, 2018) (Table 4).

The areal changes in NDMI values through the years 2015 to 2021 were used to support the result of the study (Table 4). Through the years, most of the areas in the protected landscape fall under two categories: areas with mid-high canopy cover with high water stress and areas with high canopy cover with no water stress. There has also been a noticeable increase in the areas with relatively low NDMI values indicated by red to orange pixels.

Table 4. Areal changes in NDMI values through years 2015-2021

NDMI values	Area (ha)		
	2015	2018	2021
-0.2-0 (Low canopy cover, high water stress)	4.23	22.08	16.01
0-0.2 (Average canopy cover, high water stress)	158.76	366.94	387.44
0.2-0.4 (Mid-high canopy cover, high water stress)	2128.5	1326.04	1418.39
0.4-0.6 (High canopy cover, no water stress)	1718.01	1936.41	1997
0.6 -0.8 (Very high canopy cover, no water stress)	0	355.24	189.48
0.8-1 (Total canopy cover, no water stress)	0	1.78	0.12

The 2015 NDMI showed that most of the areas in Ternate and a few in Maragondon had relatively low NDMI values. Some 4.23 ha of MPPMNGPL had low canopy cover with high water stress, while a large portion of the protected landscape (2,128.5 ha) had mid-high canopy cover with high water stress. Moreover, no areas inside the protected landscape were identified as having very high or total canopy cover with no water stress. The 2018 NDMI showed that there had been an increase in areas with low to moderate NDMI values. Additional portions were detected as having low to mid-high canopy

with water stress which could be the result of increasing disturbance because of the forest-grassland conversion from 2015 to 2018. However, it was found that 355.24 ha of forests had very high canopy cover with no water stress in 2018. The 2021 NDMI showed almost the same result as 2018; however, some areas in the protected landscape had slightly higher NDMI but were still within low to moderate values.

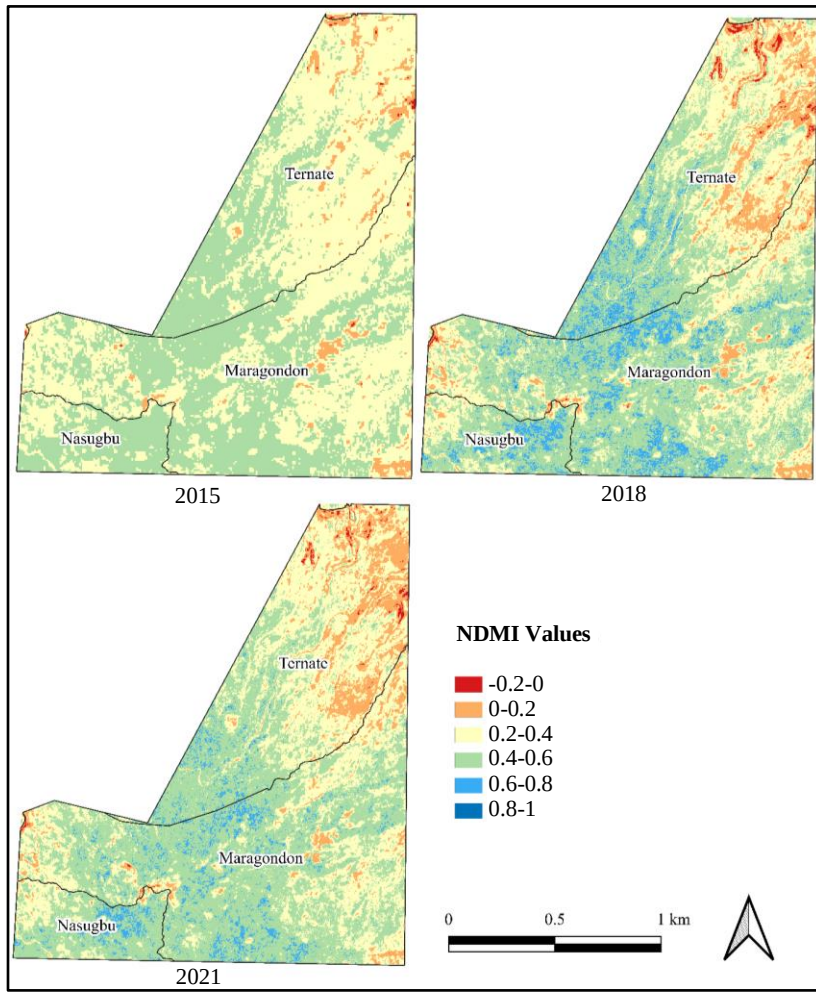

Figure 7. NDMI of MPPMNGPL in 2015, 2018 and 2021

Comparing the 2015 and 2018 NDMI images, a huge portion in the northeast of the protected landscape had lower NDMI showing disturbance over the years. It can be attributed to the forest areas being converted to grassland areas

from 2015 to 2018. In addition, some of the already disturbed areas in 2015 became more disturbed over the years. Another observation is that from 2015 to 2018, the forest areas surrounding the disturbed grasslands showed potential disturbance. It may be due to the continuous expansion of grassland areas affecting the forest. From 2018 to 2021, the potentially disturbed areas remained almost the same.

The forest experienced the largest land cover change mostly turning into grassland based on the image classification. Thus, the results of the NDMI also correspond to the results of change analysis since areas with low to moderate NDMI values were also the same areas with noticeable land cover changes in the classification.

4. Conclusion and Recommendation

The different land cover classes identified in the protected landscape were forest, grassland, built-up area, barren land and water. Although the size of forest areas decreased from 2015 to 2021, it is still the dominant land cover in the protected landscape followed by grassland. The change detection also showed the existence of land cover changes in MPPMNGPL reflecting that the forest and barren land have decreased over time while grasslands have increased. The forest showed potential disturbances based on NDMI values through the years. Given these results, there is a need to conduct further studies in the areas where disturbances have been identified. Site visits and assessments must be performed to confirm the actual causes of the land cover changes in the protected landscape.

This study provides some important lessons. First, additional and improved management efforts are necessary to alleviate the effects of anthropogenic activities inside the landscape because it is a nationally and naturally significant area. Aside from the mentioned studies stating that disturbances still occur in different terrestrial protected areas in the Philippines, this study also confirmed that there has been an apparent ineffective protected area management in the country. The conduct of land cover change analysis and detection is significant in telling the current state of MPPMNGPL in terms of the change in its land covers, which also applies to other terrestrial protected areas. Hence, the study agrees with several studies claiming how the GEE, GIS and remote sensing, when used collaboratively and effectively, can provide an ample amount of useful and accurate information.

Furthermore, the results of this study can be used by the Protected Area Management Board and stakeholders of MPPMNGPL in revising, updating, or modifying their protected area management plans. Further research about the land cover changes in the study area must be conducted for more in-depth results.

5. Acknowledgement

Special thanks are given to the Protected Area Management Board of MPPMNGPL, and Engr. Eriberta A. Estrada and Engr. Luis L. Ferma, Municipal Planning and Development Coordinators of Maragondon and Ternate, respectively, for providing the necessary documents used in the study.

6. References

Abino, A.C., Kim, S.Y., Jang, M.N., Lee, Y.J., & Chung, J.S. (2015). Assessing land use and land cover of the Marikina sub-watershed, Philippines. Forest Science and Technology, 11(2), 65-75. https://doi.org/10.1080/21580103.2014.957353

Almadrones-Reyes, K.J., & Dagamac, N.H.A. (2022). Land-use/land cover change and land surface temperature in Metropolitan Manila, Philippines using Landsat imagery. GeoJournal, 1-12. https://doi.org/10.1007/s10708-022-10701-9

Alqurashi, A., & Kumar, L. (2013). Investigating the use of remote sensing and GIS techniques to detect land use and land cover change: A review. Advances in Remote Sensing, 2, 193-204.

Angeles, L.P., Arma, E.J.M., Basaca, C.W., Biscocho, H.E.H., Castro, A.E., Cruzate, S.M., Garcia, R.J.G., Maghari, L.M.E., Pagafora, R.S., & Tadisa, E.R. (2016). Basidiomycetous fungi in Mt. Palay-Palay Protected Landscape, Luzon Island, Philippines. Asian Journal of Biodiversity, 7(1), 79-94.

Anggraeni, A., & Lin, C. (2011). Application of SAM and SVM techniques to burned area detection for Landsat TM images in forests of South Sumatra. Proceedings of the International Conference on Environmental Science and Technology, Singapore, V2160-V2164.

Antognelli, S. (2018). NDVI and NDMI vegetation indices: Instructions for use. Retrieved from https://www.agricolus.com/en/vegetation-indices-ndvi-ndmi/

Apan, A., Suarez, L.A., Maraseni, T., & Castillo, J.A. (2017). The rate, extent and spatial predictors of forest loss (2000-2012) in the terrestrial protected areas of the Philippines. Applied Geography, 81, 32-42. https://doi.org/10.1016/j.apgeog.2017.02.007

Asokan, A., & Anitha, J.J.E.S.I. (2019). Change detection techniques for remote sensing applications: A survey. Earth Science Informatics, 12(2), 143-160. https://doi.org/10.1007/s12145-019-00380-5

Baamonde, S., Cabana, M., Sillero, N., Penedo, M.G., Naveira, H., & Novo, J. (2019). Fully automatic multi-temporal land cover classification using Sentinel-2 image data. Procedia Computer Science, 159, 650-657. https://doi.org/10.1016/j.procs.2019.09.220

Barakat, A., Khellouk, R., El Jazouli, A., Touhami, F., & Nadem, S. (2018). Monitoring of forest cover dynamics in the eastern area of Béni-Mellal Province using ASTER and Sentinel-2A multispectral data. Geology, Ecology, and Landscapes, 2(3), 203-215. https://doi.org/10.1080/24749508.2018.1452478

Berca, M., & Horoiaș, R. (2022). NDMI use in recognition of water stress issues, related to winter wheat yields in Southern Romania. Scientific Papers: Management, Economic Engineering in Agriculture and Rural Development, 22(2), 105-112.

Brandt, P., Hamunyela, E., Herold, M., De Bruin, S., Verbesselt, J., & Rufino, M.C. (2018). Sustainable intensification of dairy production can reduce forest disturbance in Kenyan montane forests. Agriculture, Ecosystems and Environment, 265, 307-319. https://doi.org/10.1016/j.agee.2018.06.011

Brebante, B.M. (2017). Analyzing the effects of land cover/land use changes on flashflood: A case study of Marikina River Basin (MRB), Philippines (Master's Thesis). Faculty of Geo-Information Science and Earth Observation, University of Twente, Enschede, Netherlands.

Carandang, A.P., Bugayong, L.A., Dolom, P.C., Garcia, L.N., Villanueva, M.B., & Espirit, N.O. (2013). Analysis of key drivers of deforestation and forest degradation in the Philippines. Bonn, Germany: Deutsche Gesellschaft für Internationale Zusammenarbeit (GIZ) GmbH.

Causaren, R.M. (2016). Species diversity, abundance, and habitat distribution of anurans in Mts. Palay-Palay Mataas-na-Gulod Protected Landscape, Luzon Island, Philippines. Philippine Journal of Systematic Biology, 10, 63-76.

Causaren, R.M., Diesmos, A.C., & Mallari, N.A. (2016). Anuran diversity and ecology from forest fragments in Cavite Province, Luzon Island, Philippines. Philippine Journal of Systematic Biology, 10, 52-62.

Ceccato, P., Flasse, S., Tarantola, S., Jacquemoud, S., & Grégoire, J.M. (2001). Detecting vegetation leaf water content using reflectance in the optical domain. Remote Sensing of Environment, 77(1), 22-33. https://doi.org/10.1016/S0034-4257(01)00191-2

Chaves, M., Picoli, M.C.A., & Sanches, I.D. (2020). Recent applications of Landsat 8/OLI and Sentinel-2/MSI for land use and land cover mapping: A systematic review. Remote Sensing, 12(18), 3062. https://doi.org/10.3390/rs12183062

Chen, N., Tsendbazar, N.E., Hamunyela, E., Verbesselt, J., & Herold, M. (2021). Sub-annual tropical forest disturbance monitoring using harmonized Landsat and Sentinel-2 data. International Journal of Applied Earth Observation and Geoinformation, 102, 102386. https://doi.org/10.1016/j.jag.2021.102386

Congalton, R.G. (1991). A review of assessing the accuracy of classifications of remotely sensed data. Remote Sensing of Environment, 37(1), 35-46. https://doi.org/10.1016/0034-4257(91)90048-B

Congalton, R.G., & Green, K. (2019). Assessing the accuracy of remotely sensed data: Principles and practices. Florida, United States: CRC Press.

Congedo, L. (2021). Semi-Automatic Classification Plugin: A Python tool for the download and processing of remote sensing images in QGIS. Journal of Open Source Software, 6(64), 3172.

Department of Environment and Natural Resources Mines and Geosciences Bureau (MGB) Region 4-A. (2021). 2021 CALABARZON provincial profile. Retrieved from https://drive.google.com/file/d/1VzVNvFNgTkZYF2koY_5C9H1tzcfAvza1/view

Doyog, N.D., Lumbres, R.I.C., & Baoanan, Z.G. (2021). Monitoring of land use and land cover changes in Mt. Pulag National Park using Landsat and Sentinel imageries. Philippine Journal of Science, 150(4), 721-732.

Dumago, S.W.L., Puno, G.R., & Ingotan, S.S. (2018). Water quality assessment in various land use and land cover of Muleta watershed Bukidnon, Philippines. Journal of Biodiversity and Environmental Sciences, 12(3), 201-209.

Eskandari, S., Reza Jaafari, M., Oliva, P., Ghorbanzadeh, O., & Blaschke, T. (2020). Mapping land cover and tree canopy cover in Zagros forests of Iran: Application of Sentinel-2, Google Earth, and field data. Remote Sensing, 12(12), 1912. https://doi.org/10.3390/rs12121912

Esri. (2022). Sentinel-2 land use/land cover time series. Retrieved from https://env1.arcgis.com/arcgis/rest/services/Sentinel2_10m_LandCover/ImageServer

Google. (2022). Google Earth Pro [Computer software]. Retrieved from https://www.google.com/earth/versions/#download-pro

Grigoraș, G., & Urițescu, B. (2019). Land use/land cover changes dynamics and their effects on surface urban heat island in Bucharest, Romania. International Journal of Applied Earth Observation and Geoinformation, 80, 115-126.

Halefom, A., Teshome, A., Sisay, E., Khare, D., Dananto, M., Singh, L., & Tadesse, D. (2018). Applications of remote sensing and gis in land use/land cover change detection: A case study of Woreta Zuria watershed, Ethiopia. Applied Research Journal of Geographic Information System, 1(1), 1-9.

Hamunyela, E., Brandt, P., Shirima, D., Do, H.T.T., Herold, M., & Roman-Cuesta, R. M. (2020). Space-time detection of deforestation, forest degradation, and regeneration in montane forests of Eastern Tanzania. International Journal of Applied Earth Observation and Geoinformation, 88, 102063. https://doi.org/10.1016/j.jag.2020.102063

Haque, M.I., & Basak, R. (2017). Land cover change detection using GIS and remote sensing techniques: A spatio-temporal study on Tanguar Haor, Sunamganj, Bangladesh. The Egyptian Journal of Remote Sensing and Space Science, 20(2), 251-263. https://doi.org/10.1016/j.ejrs.2016.12.003

Janiola, M.D.C., & Puno, G.R. (2018). Land use and land cover (LULC) change detection using multitemporal Landsat imagery: A case study in Allah Valley Landscape in Southern Philippines. Journal of Biodiversity and Environmental Science, 12(2), 98-108.

Klemas, V., & Smart, R. (1983). The influence of soil salinity, growth form, and leaf moisture on-the spectral radiance of *Spartina alterniflora* canopies. Photogrammetric Engineering and Remote Sensing, 49, 77-83.

Korhonen, L., Packalen, P., & Rautiainen, M. (2017). Comparison of Sentinel-2 and Landsat 8 in the estimation of boreal forest canopy cover and leaf area index. Remote Sensing of Environment, 195, 259-274. https://doi.org/10.1016/j.rse.2017.03.021

Kruse, F.A. (1994). Imaging spectrometer data analysis: A tutorial. Retrieved from https://citeseerx.ist.psu.edu/document?repid=rep1&type=pdf&doi=a43fa4dd41bc947035be0cee5c42284f765230b6

Lagat, R.D., & Causaren, R.M. (2019). Initial terrestrial vertebrate diversity assessment in upland Cavite, Philippines. Philippine Journal of Systematic Biology, 12(2), 70-91.

Li, J., & Roy, D.P. (2017). A global analysis of Sentinel-2A, Sentinel-2B and Landsat-8 data revisit intervals and implications for terrestrial monitoring. Remote Sensing, 9(9), 902. https://doi.org/10.3390/rs9090902

Lima, T.A., Beuchle, R., Langner, A., Grecchi, R. C., Griess, V.C., & Achard, F. (2019). Comparing Sentinel-2 MSI and Landsat 8 OLI imagery for monitoring selective logging in the Brazilian Amazon. Remote Sensing, 11(8), 961. https://doi.org/10.3390/rs11080961

Liu, C., Frazier, P., & Kumar, L. (2007). Comparative assessment of the measures of thematic classification accuracy. Remote Sensing of Environment, 107(4), 606-616. https://doi.org/10.1016/j.rse.2006.10.010

Mallari, N.A.D., & Tabaranza, B.R. (2001). Key conservation sites in the Philippines: A Haribon Foundation & BirdLife International directory of important bird areas. Makati City, Philippines: Bookmark Incorporated.

Medecilo, M.M.P., & Lagat, M.N. (2017). Floristic composition of the remaining forest in upland Cavite, Luzon Island, Philippines. Philippine Journal of Systematic Biology, 11(1), 74-94.

Municipality of Maragondon. (2013). Mt. Palaypalay/Mataas na Gulod. Retrieved from http://maragondon-official.cavite.gov.ph/index.php/tourism/naturetrip/66-mt-palaypalay-mataas-na-gulod

Municipality of Ternate. (n.d.) The comprehensive land use plan. Municipality of Ternate, Cavite, Philippines.

National Economic and Development Authority. (2008). Regional physical framework plan 2004-2030. Retrieved from https://rdccalabarzon.gov.ph/assets/files/RPFP/RPFP-2004-2030%20vol%202.pdf

Ochtyra, A., Marcinkowska-Ochtyra, A., & Raczko, E. (2020). Threshold-and trend-based vegetation change monitoring algorithm based on the inter-annual multi-temporal normalized difference moisture index series: A case study of the Tatra Mountains. Remote Sensing of Environment, 249, 112026. https://doi.org/10.1016/j.rse.2020.112026

Perumal, K., & Bhaskaran, R. (2010). Supervised classification performance of multispectral images. arXiv. https://doi.org/10.48550/arXiv.1002.4046

Philippine Atmospheric, Geophysical and Astronomical Services Administration. (n.d.). Climate of the Philippines. Retrieved from https://www.pagasa.dost.gov.ph/information/climate-philippines

Philippine Official Gazette. (1975). Proclamation No. 1520, s. 1975. Retrieved from https://www.officialgazette.gov.ph/1975/11/28/proclamation-no-1520-s-1975/

Philippine Official Gazette. (2007). Proclamation No. 1315, s. 2007. Retrieved from https://www.officialgazette.gov.ph/2007/06/27/proclamation-no-1315-s-2007/

Praticò, S., Solano, F., Di Fazio, S., & Modica, G. (2021). Machine learning classification of Mediterranean forest habitats in Google Earth Engine based on seasonal Sentinel-2 time-series and input image composition optimisation. Remote Sensing, 13(4), 586. https://doi.org/10.3390/rs13040586

Province of Cavite. (2020). Cavite ecological profile 2020. Retrieved from https://cavite.gov.ph/home/cavite-ecological-profile-2020/

QGIS Development Team. (2020). QGIS Geographic Information System [Computer software]. Retrieved from https://www.qgis.org/en/site/forusers/download.html

Sánchez-Espinosa, A., & Schröder, C. (2019). Land use and land cover mapping in wetlands one step closer to the ground: Sentinel-2 versus Landsat 8. Journal of Environmental Management, 247, 484-498. https://doi.org/10.1016/j.jenvman.2019.06.084

Shah, S.A., & Kiran, M. (2021). A GIS-based technique analysis of land use and land cover change detection in taluka Mirpur Mathelo: A case study in district Ghotki, Pakistan. International Advanced Researches and Engineering Journal, 5(2), 231-239.

Soriano, M., Hilvano, N., Garcia, R., Hao, A.J., Alegre, A., & Tiburan, C., Jr. (2019). Land use/land cover change detection and urban sprawl analysis in the Mount Makiling

Forest Reserve watersheds and buffer zone, Philippines. Environments, 6(2), 9. https://doi.org/10.3390/environments6020009

Thanh, H.N.T., Doan, T.M., Tomppo, E., & McRoberts, R.E. (2020). Land use/land cover mapping using multitemporal sentinel-2 imagery and four classification methods – A case study from Dak Nong, Vietnam. Remote Sensing, 12(9), 1367. https://doi.org/10.3390/rs12091367

Thomlinson, J.R., Bolstad, P.V., & Cohen, W.B. (1999). Coordinating methodologies for scaling landcover classifications from site-specific to global: Steps toward validating global map products. Remote Sensing of Environment, 70(1), 16-28. https://doi.org/10.1016/S0034-4257(99)00055-3

Tu, B., Zhou, C., Kuang, W., Guo, L., & Ou, X. (2018). Hyperspectral imagery noisy label detection by spectral angle local outlier factor. IEEE Geoscience and Remote Sensing Letters, 15(9), 1417-1421. https://doi.org/10.1109/LGRS.2018.2842792

United States Geological Survey. (2021). Normalized Difference Moisture Index. Retrieved from https://www.usgs.gov/landsat-missions/normalized-difference-moisture-index

Verma, R., & Garg, P.K. (2019). Remote sensing based building indexing approach in relation to urban heat island. In A. Agrawal & R. Gupta (Eds.), Proceedings of the 53rd International Conference of the Architectural Science Association, Roorkee, India, 666-674.

Verma, P., Raghubanshi, A., Srivastava, P.K., & Raghubanshi, A.S. (2020). Appraisal of kappa-based metrics and disagreement indices of accuracy assessment for parametric and nonparametric techniques used in LULC classification and change detection. Modeling Earth Systems and Environment, 6(2), 1045-1059. https://doi.org/10.1007/s40808-020-00740-x

Wilson, E.H., & Sader, S.A. (2002). Detection of forest harvest type using multiple dates of Landsat TM imagery. Remote Sensing of Environment, 80(3), 385-396. https://doi.org/10.1016/S0034-4257(01)00318-2

Yadav, Y., Chhetri, B.B.K., Raymajhi, S., RajTiwari, K., & Sitaula, B.K. (2019). Dynamics of land use land cover change and mapping of tree outside forest (TOF) in Terai, Nepal. International Journal of Environmental Science and Technology, 19(1), 4-9. https://doi.org/10.19080/IJESNR.2019.18.556002

Yan, L., & Roy, D.P. (2018). Large-area gap filling of Landsat reflectance time series by spectral-angle-mapper based spatio-temporal similarity (SAMSTS). Remote Sensing, 10(4), 609. https://doi.org/10.3390/rs10040609

Yiqiang, G., Yanbin, W., Zhengshan, J., Jun, W., & Luyan, Z. (2010). Remote sensing image classification by the Chaos Genetic Algorithm in monitoring land use changes. Mathematical and Computer Modelling, 51(11-12), 1408-1416. https://doi.org/10.1016/j.mcm.2009.10.023

Wang, D., Wan, B., Qiu, P., Su, Y., Guo, Q., Wang, R., ... Wu, X. (2018). Evaluating the performance of Sentinel-2, Landsat 8 and Pléiades-1 in mapping mangrove extent and species. Remote Sensing, 10(9), 1468. https://doi.org/10.3390/rs10091468